



Structural, chemical bonding, electronic and magnetic properties of KMF_3 ($M = \text{Mn, Fe, Co, Ni}$) compounds



Hayatullah^a, G. Murtaza^{b,*}, R. Khenata^c, S. Muhammad^a, A.H. Reshak^{d,e}, Kin Mun Wong^f, S. Bin Omran^g, Z.A. Alahmed^g

^a Materials Modeling Lab, Department of Physics, Hazara University, Mansehra, Pakistan

^b Materials Modeling Lab, Department of Physics, Islamia College University, Peshawar, Pakistan

^c LPQ3M Laboratory, Institute of Science and Technology, University of Mascara, Algeria

^d New Technologies - Research Center, University of West Bohemia, Univerzitni 8, 306 14 Pilsen, Czech Republic

^e Center of Excellence Geopolymer and Green Technology, School of Material Engineering, University Malaysia Perlis, 01007 Kangar, Perlis, Malaysia

^f Institut für Physik & IMN MacroNano[®] (ZIK), Technische Universität Ilmenau, Prof. Schmidt-Str. 26, Ilmenau 98693, Germany

^g Department of Physics and Astronomy, King Saud University, P.O. Box 2455, Riyadh 11451, Saudi Arabia

ARTICLE INFO

Article history:

Received 16 November 2013

Accepted 29 December 2013

Available online 24 January 2014

Keywords:

Ferroperovskites

DFT

Electronic properties

Magnetic properties

ABSTRACT

KMF_3 ($M = \text{Mn, Fe, Co, Ni}$) compounds crystallize in the cubic perovskite structure with space group $Pm\bar{3}m$ (#221) at ambient conditions. Structural, chemical bonding, electronic and magnetic properties of these compounds are investigated using the full-potential linearized augmented plane wave (FP-LAPW) method within the density functional theory (DFT). The calculated structural parameters agree well with the experimental measurements. From the elastic properties, it is inferred that these compounds are elastically stable. Moreover, KMnF_3 is found to be ductile in nature while the remaining compounds are brittle. The results of the electronic band structure show that KMnF_3 and KNiF_3 are indirect band gap semiconductors in both spin channels, while KFeF_3 and KCoF_3 are half metallic, being semiconductors with majority spin channel and metals with spin minority channel. The bonding behavior of the studied compounds is expressed as a combination of covalent–ionic behavior. The magnetic study reveals the ferromagnetic behavior for these compounds. The half metallicity and the ferromagnetic behavior favor these compounds for spintronic applications.

© 2014 Elsevier B.V. All rights reserved.

1. Introduction

The field of spintronics is concerned with the search of highly spin polarized materials for enhancing the tunneling magneto resistance (TMR) of magnetic tunnel junctions (MTJs), which are active members for the magnetic random access memory (MRAM) elements. There are two ways for achieving a spin polarization, employing half metals or exploiting spin filtering effect. The half metals, Heusler alloys, and magnetic perovskites have been intensively studied for finding the electronic, magnetic and optoelectronic properties [1]. First principles-based methods (ab initio methods) which use only the atomic constants as input parameters to solving the Schrödinger equation have now become the most powerful probes for predicting the ground state properties of materials without any adjustable parameters [2].

Materials possessing perovskite structure have received enormous attention over the past two decades because of their interesting properties such as high temperature superconductivity and

colossal magneto resistivity [3]. Perovskite materials show a high degree of magnetic properties due to their particular ordering of occupied d-orbital. The halogen-based cubic perovskite crystals ABX_3 (where A and B are cations and X is a monovalent halogen anion) are a subject of numerous theoretical and experimental studies due to combination of their relatively simple crystal structure, easiness of preparations and doping with different impurity ions and variety of other electrical, optical and magnetic properties [4].

Among them, KMF_3 ($M = \text{Mn, Fe, Co, Ni}$ and Zn) perovskites have been in the limelight in these days and have been actively researched due to their high-temperature super-ionic behavior and physical properties such as piezoelectric characteristics, ferromagnetism, nonmagnetic insulator behavior [5–7]. It is well known that alkali metal fluorides have wide applications in the organo fluorine chemistry both as a fluorinating agent as well as a catalyst in various reactions [8,9].

The alkali metal fluorides KMF_3 ($M = \text{Mn, Fe, Co}$ and Ni) have cubic crystal structure, with space group $Pm\bar{3}m$ (No. 221) [10–12]. Our calculations are based on the density functional theory using generalized gradient approximation (GGA). Calculated ground-state structural properties of the aforementioned crystals have

* Corresponding author. Tel.: +92 321 6582416.

E-mail address: murtaza@icp.edu.pk (G. Murtaza).

been compared with the available theoretical and experimental data.

2. Method of calculation

In the present work the Kohn–Sham equation [13] is solved to calculate the structural, elastic, electronic and magnetic of the cubic perovskites KMF_3 ($M = \text{Mn, Fe, Co and Ni}$). The Kohn–Sham equation in atomic units is;

$$[T_s[\rho] + V_{ee}[\rho] + V_{en}[\rho] + V_{xc}[\rho]]\phi_i(\vec{r}) = \epsilon_i\phi_i(\vec{r}) \quad (1)$$

The first term on the left hand side represents the kinetic energy of non-interacting electrons and the second term is the classical Coulomb interaction of electrons. The third term is the external effective potential from the fixed nuclei and the fourth term is the exchange correlation potential.

The Kohn–Sham equation is solved iteratively till self-consistency is achieved. Iteration cycles are needed because of interdependency between orbitals and potentials. In the Kohn–Sham scheme the electron density can be obtained by summing over all the occupied states [13]. The electron density is given by the following expression [14];

$$\rho(\vec{r}) = \sum_i^N f_i |\phi_i(\vec{r})|^2 \quad (2)$$

where f_i is the occupation and $\phi_i(\vec{r})$ is the wave function of the i th orbital. The full potential linearized augmented plane wave (FP-LAPW) method [15,16] with Wu and Cohen generalized gradient approximation [17] is used to solve Eq. (1). In the generalized gradient scheme, the exchange–correlation energy (E_{xc}) is a function of the local electron spin densities and their gradients:

$$E_{xc}^{GGA}(\rho_\uparrow, \rho_\downarrow) = \int E_{xc}(\rho_\uparrow(\vec{r}), \rho_\downarrow(\vec{r}), \nabla\rho_\uparrow(\vec{r}), \nabla\rho_\downarrow(\vec{r}))d^3r \quad (3)$$

where $\rho_\uparrow, \rho_\downarrow, \nabla\rho_\uparrow, \nabla\rho_\downarrow$ are the densities and the gradient of densities for spin up and spin down electrons. E_{xc} is the exchange–correlation energy per particle. The spin polarized FP-LAPW method used for the computation of the ground state properties of materials [18] was started by the structural optimization of the crystal structure of the material using wien2k software [19]. In the full potential scheme, the wave function, the potential and charge density are expanded into two different basis. The wave function is expanded in spherical harmonics in the atomic spheres while outside the spheres (interstitial regions) it is expanded in plane wave basis. The potential is also expanded in the same manner:

$$V(r) = \begin{cases} \sum_{lm} V_{lm}(r)Y_{lm}(r) & \text{(a)} \\ \sum_k V_k e^{ikr} & \text{(b)} \end{cases} \quad (4)$$

where Eqs. (4)(a) and (4)(b) are for inside and outside atomic sphere, respectively. Inside the sphere the maximal value for the wave function expansion l is set to be 10 and it is symmetric, while outside the sphere it is constant. The muffin-tin radii (R_{MT}) are chosen in such a way that there is no charge leakage from the core. The (R_{MT}) were taken to be 2.5, 1.98, 1.95, 1.93, 1.90 and 1.72 (a.u.) for K, Mn, Fe, Co, Ni and F, respectively. The wave functions in the interstitial region were expanded in plane waves with a cut-off $R_{MT} * K_{max} = 7$, where R_{MT} denotes the smallest muffin-tin radius and K_{max} gives the magnitude of the largest K vector in the plane wave expansion. For the structural properties the integrals over the Brillouin zone are performed up to 35 k -points for GGA using the modified tetrahedron method [20]. For the calculations of the electronic and magnetic properties, a dense mesh of uniformly

distributed k -points is required. Hence, the Brillouin zone integration was performed with 2000 k -points.

3. Results and discussion

3.1. Structural properties

Our aim in this section is to calculate the total energy as a function of unit-cell volume to obtain the ground state properties of KMF_3 ($M = \text{Mn, Fe, Co and Ni}$) compounds. In the cubic unit cell of the perovskites K is placed at (0, 0, 0), M at (1/2, 1/2, 1/2) and F at (1/2, 1/2, 0), (1/2, 0, 1/2) and (0, 1/2, 1/2) sites. The volume of the unit cell of each KMF_3 ($M = \text{Mn, Fe, Co and Ni}$) is optimized to obtain the structural properties such as the lattice constant a , the bulk modulus B , and the ground state energy E_0 . In the optimization procedure, the total energy of each unit cell is calculated by varying the unit cell volume and fitted by Birch–Murnaghan's equation of state [21]. The ground state energy (E_0), is the minimum energy of the unit cell and the volume corresponding to this energy is the ground state volume. The calculated values of these parameters are compared with the available theoretical and experimental results in Table 1. Furthermore, the lattice constants are also calculated by ionic radii using the following empirical formula [22];

$$a = \alpha + \beta(r_k + r_F) + \gamma(r_X + r_F) \quad (5)$$

where α (0.06741), β (0.4905) and γ (1.2921) [22] are constants and r_k is the ionic radius of K (1.64 Å) [22], r_F is the ionic radius of F (1.285 Å) and r_X is the ionic radius of Mn (0.53 Å), Fe (0.78), Co (0.745) and Ni (0.69) [22]. The calculated lattice constants for the studied materials are also quoted in Table 1. As a common feature with the previous results, it is seen that our calculated lattice constants are slightly underestimated within 0.21%, 1.69%, 1.3% and 0.54% for KMnF_3 , KFeF_3 , KCoF_3 and KNiF_3 , respectively, compared to the experimental data [23]. These small discrepancies could be attributed to the fact that the present calculation pertains to $T = 0$ K, whereas the experimental measurement were performed at room temperature. Our calculated values of lattice constants for KMF_3 ($M = \text{Mn, Fe, Co and Ni}$) are in good agreement with the available theoretical results [12]. The bulk modulus B is a measure of the crystal rigidity, thus a large B is for high crystal rigidity. In view of Table 1, KFeF_3 is harder and less compressible than KNiF_3 , KCoF_3 and KMnF_3 . Bond length plays an important role in the symmetry of perovskite structures. The calculated bond lengths from cation to anions ($M - F, K - F, K - M$) are listed in Table 2. The calculated bond length can help to compute the tolerance factor for perovskite crystals using the following expression [24],

$$t = \frac{0.707((K - F))}{(M - F)} \quad (6)$$

where $\langle K - F \rangle$ and $\langle M - F \rangle$ are the average bond lengths in these perovskites. Our calculated tolerance factor values are in good agreement to the analytically calculated-ones [25]. For cubic perovskites the tolerance factor generally lies between 0.95 and 1.04 [26]. Our computed results listed in Table 2 are included in this energy range, revealing the cubic perovskite structure for KMF_3 ($M = \text{Mn, Fe, Co and Ni}$) compounds. As a result our calculated values of structural parameters are in good agreement with the available experimental and theoretical results which confirms validity and reliability of the performed calculations.

3.2. Elastic properties

The elastic constants are important parameters to describe the response of the materials to an applied macroscopic stress. These constants play an important role in providing valuable information

Table 1

Calculated lattice constants a (Å), bulk moduli B (GPa), elastic constants C_{ij} (in GPa), shear modulus G (GPa), Young's modulus E (GPa), Poisson's ratios, ν , anisotropy factor A , B/G ratio and Kleinman parameter, ζ , at equilibrium volume for KMF_3 ($M = \text{Mn, Fe, Co and Ni}$) compared with other theoretical and experimental results.

	Present work	Present work (analytical)	Experimental work	Other work
<i>KMnF₃</i>				
a_0	4.193	4.235	4.202 ^a	4.188 ^b
B	70.1			
C_{11}	69.26			
C_{12}	23.57			
C_{44}	8.36			
E	35.28			
G	13.08			
ν	0.35			
A	0.37			
B/G	2.97			
ζ	0.48			
<i>KFeF₃</i>				
a_0	4.061	4.170	4.13 ^a	4.124 ^b
B	93.28			
C_{11}	94.48			
C_{12}	21.98			
C_{44}	30.88			
E	79.81			
G	32.93			
ν	0.21			
A	0.85			
B/G	1.40			
ζ	0.38			
<i>KCoF₃</i>				
a_0	4.041	4.125	4.094 ^a	4.076 ^b
B	83.04			
C_{11}	116.80			
C_{12}	24.83			
C_{44}	40.53			
E	102.91			
G	42.64			
ν	0.20			
A	0.88			
B/G	1.37			
ζ	0.41			
<i>KNiF₃</i>				
a_0	4.012	4.054	4.034 ^a	4.0118 ^b
B	89.26			
C_{11}	115.73			
C_{12}	53.85			
C_{44}	41.63			
E	95.14			
G	36.96			
ν	0.2			
A	1.35			
B/G	2.01			
ζ	0.59			

^a Ref. [23].

^b Ref. [12].

on the stability and stiffness of materials. Since the studied compounds have cubic symmetry, we need to calculate only three independent elastic parameters namely C_{11} , C_{12} , and C_{44} to completely characterize the mechanical properties. Hence, a set of three equations is needed to determine all these constants.

The first equation involves calculating the bulk modulus (B), which is given by [27]:

$$B = 1/3(C_{11} + 2C_{12}) \quad (7)$$

The second equation involves performing volume-conserving tetragonal strain tensor ε .

$$\vec{\varepsilon} = \begin{pmatrix} \varepsilon & 0 & 0 \\ 0 & \varepsilon & 0 \\ 0 & 0 & \frac{1}{(1+\varepsilon)^2} - 1 \end{pmatrix} \quad (8)$$

Table 2

Calculated bond lengths and tolerance factor for KMF_3 ($M = \text{Mn, Fe, Co and Ni}$).

	Present work	Other work
<i>KMnF₃</i>		
Bond length K–F	2.9503	
Mn–F	2.0862	
K–Mn	3.6134	
Tolerance factor	0.9998	0.978 ^a
<i>KFeF₃</i>		
Bond length K–F	2.9139	
Fe–F	2.0604	
K–Fe	3.5688	
Tolerance factor	0.9999	1.002 ^a
<i>KCoO₃</i>		
Bond length K–F	2.8299	
Co–F	2.0009	
K–Co	3.4683	
Tolerance factor	0.9999	1.019 ^a
<i>KNiF₃</i>		
Bond length		
K–F	2.3009	
Ni–F	1.9731	
K–Ni	3.4322	
Tolerance factor	0.8244	1.047 ^a

^a Ref. [26].

Application of this strain changes the total energy from its unstrained value to:

$$E(\varepsilon) = (C_{11} - C_{12})3V_0\varepsilon^2 + O(\varepsilon^2) \quad (9)$$

where V_0 is the volume of the unit cell.

Lastly, we used the volume-conserving rhombohedral strain tensor given by:

$$\vec{\varepsilon} = \frac{\varepsilon}{3} \begin{pmatrix} 1 & 1 & 1 \\ 1 & 1 & 1 \\ 1 & 1 & 1 \end{pmatrix} \quad (10)$$

which change the total energy to

$$E(\varepsilon) = E(0) + \frac{1}{6}(C_{11} + 2C_{12} + 4C_{44})V_0\varepsilon^2 + O(\varepsilon^3) \quad (11)$$

The computed values of the elastic constants for $KMnF_3$ ($M = \text{Mn, Fe, Co and Ni}$) compounds are given in Table 1. In view on Table 1, one can notice that the unidirectional elastic constant C_{11} , which is related to the unidirectional compression along the principal crystallographic directions, is about 87.93% higher than C_{44} for $KMnF_3$, 67.32% for $KFeF_3$, 65.29% for $KCoF_3$ and 64.04% for $KNiF_3$, indicating that these compounds present a weaker resistance to the pure shear deformation compared to the resistance to the unidirectional compression. It is known that the elastic constants are related to the bulk modulus value by the relation (7) and since the true experimental values of the bulk modulus and the elastic constants of the herein studied compounds are not available, the magnitude of the deviation of our calculated elastic moduli is difficult to estimate. It may be assumed to be small, since the calculations are performed with a large number of k -points and a large number of plane waves. It is worthy to mention here that in general, it is far to say that the experimental data are well reproduced by the calculation. On reason for this difference is that in the theoretical calculations the crystal is assumed to be at $T = 0$ K and thus do not include contributions from lattice vibrations that are present at room temperature measurements. Finite temperature generally tends to reduce the elastic constant values due to the thermal expansion, as also found theoretically and experimentally for fluoro-perovskites $KZnF_3$, $KMgF_3$ and $CsCdF_3$ [44–46]. To the

best of our knowledge no experimental or theoretical value for the elastic constants has been reported; hence our results can serve as a prediction for future investigations.

The requirement of mechanical stability in a cubic structure leads to the following restrictions on the elastic constants [31]:

$$\frac{1}{3}(C_{11} + 2C_{12}) > 0; \quad C_{44} > 0; \quad \frac{1}{2}(C_{11} - C_{12}) > 0; \quad C_{12} < B < C_{11} \quad (12)$$

These criteria are satisfied, indicating that these compounds are elastically stable.

As a matter of fact, the elastic anisotropy of crystals has an important implication in engineering science since it is highly correlated with the possibility to induce micro cracks in materials [32]. To quantify the elastic anisotropy, we have computed the anisotropy factor “ $A = 2C_{44}/(C_{11} - C_{12})$ ” from the present values of the elastic constants. The anisotropy factor A gives information about the anisotropy: for $A = 1$, the material is considered to be a completely isotropic, while any value smaller or larger than 1 indicates anisotropy of these compounds. The magnitude of the deviation from 1 is a measure of the degree of elastic anisotropy possessed by the crystal. From the computed anisotropy values listed in Table 1, one can conclude that KNiF_3 is highly isotropic, while KMnF_3 shows large elastic anisotropy and KFeF_3 , KCoF_3 show small anisotropy.

The knowledge of the single-crystal elastic constants C_{ij} allows the calculation of some polycrystalline elastic moduli, such as the shear modulus G , the Young’s modulus E and the Poisson’s ratio ν , using the Voigt–Reus–Hill approximations by the following expression [33–36]:

$$E = \frac{9BG}{3B + G} \quad (13)$$

$$\nu = \frac{3B - 2G}{2(3B + G)} \quad (14)$$

$$G_V = \frac{1}{5}(C_{11} - C_{12} + 3C_{44}) \quad (15)$$

$$G_R = \frac{5C_{44}(C_{11} - C_{12})}{4C_{44} + 3(C_{11} - C_{12})} \quad (16)$$

Another important elastic parameter is that of Kleinman parameter ζ which describes the relative positions of cation and anion sub-lattices under the volume-conserving strain distortions for which positions are not fixed by symmetry [37]. This parameter is calculated by the following equation;

$$\zeta = \frac{C_{11} + 8C_{12}}{7C_{11} + 2C_{12}} \quad (17)$$

The calculated values of the mentioned elastic moduli for polycrystalline KMnF_3 ($M = \text{Mn, Fe, Co and Ni}$) compounds are quoted in Table 1. The Young’s modulus (E) is a good indicator about the stiffness of the material. When it is higher for a given material, the material seems to be stiffer. From the present results of E , we can state that KCoF_3 is stiffer than KNiF_3 , KFeF_3 and KMnF_3 . Poisson’s ratio provides further information for dealing with the characteristic of the bonding forces than any of the other elastic property. 0.25 and 0.5 values are the lower and the upper limits for central force in solids, respectively [38]. The calculated values of Poisson’s ratio for KMnF_3 , KFeF_3 , KCoF_3 and KNiF_3 are 0.35,

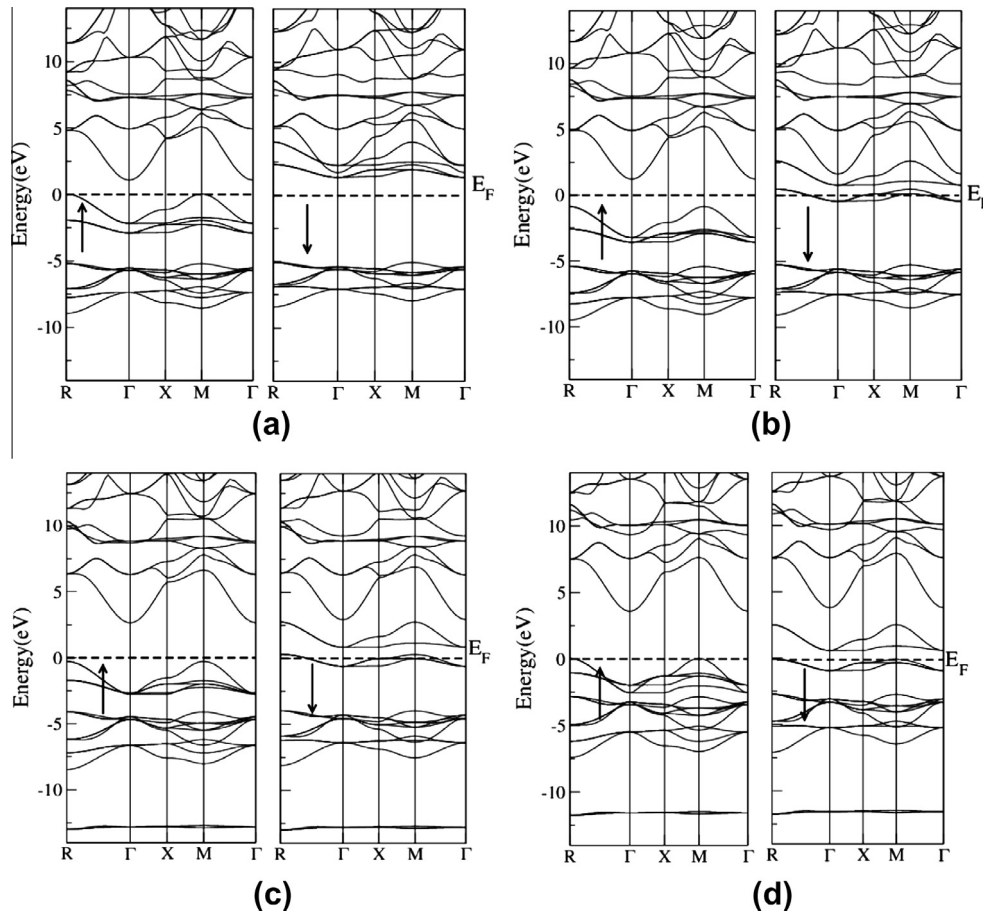


Fig. 1. Electronic band structure (spin up is represented by up arrow and vice versa) for KMnF_3 (a), KFeF_3 (b), KCoF_3 (c) and KNiF_3 (d).

0.21, 0.21 and 0.20, respectively. Thus, the high Poisson's value for KMnF_3 indicates that interatomic forces in this compound are central.

It is known that a small value of Kleinman parameter implies there is a large resistance against bond bending or bond angle distortion and vice versa [39,40]. From Table 1 this value is 0.48, 0.38, 0.41 and 0.59 for KMnF_3 , KFeF_3 , KCoF_3 and KNiF_3 , respectively, meaning that KFeF_3 is more resistant to bond bending or bond angle distortions compared to KCoF_3 , KMnF_3 and KNiF_3 . Cauchy pressure ($C_{12} - C_{44}$), Pugh's index of ductility (B/G) and Poisson's ratio (ν) are factors which allow us to know the ductile/brittle nature of a given material. The Cauchy's pressure, defined as the difference between the two particular elastic constants $C_{12} - C_{44}$ is considered to serve as an indication of ductility: if the pressure is positive (negative), the material is expected to be ductile (brittle) [41]. Here the value of the Cauchy's pressure is positive for KMnF_3 and KNiF_3 and it is negative for KFeF_3 and KCoF_3 which clearly highlights the ductile and brittle nature of these compounds, respectively. Another index of ductility is the (B/G) ratio. According to Pugh's [42] ratio, the high (low) B/G ratio is associated with the ductile

(brittle) nature of the materials. The critical value which separates the ductile and brittle was found to be 1.75. As displayed in Table 1, the calculated B/G ratio is larger than the critical value for KMnF_3 and KNiF_3 and smaller for KFeF_3 and KCoF_3 which also confirms that latter compounds are brittle in nature. We may also refer to Frantsevich et al. [43] who distinguish the ductility and brittleness of materials in terms of Poisson's ratio (ν). According to Frantsevich rule, the critical value of material is 0.26. For brittle materials, the Poisson's ratio is less than 0.26; otherwise the material behaves in a ductile manner as recently demonstrated in a study of brittle versus ductile transition in some perovskites compounds from first-principle calculations [28–30]. Here, the calculated Poisson's ratio for KMnF_3 is larger than (0.26) while it is less than (0.26) for KNiF_3 , KFeF_3 and KCoF_3 categorizing the latter compounds as ductile brittle materials.

3.3. Electronic properties

To illustrate the corresponding electronic properties, the spin resolved band structure, total and partial density of states are given

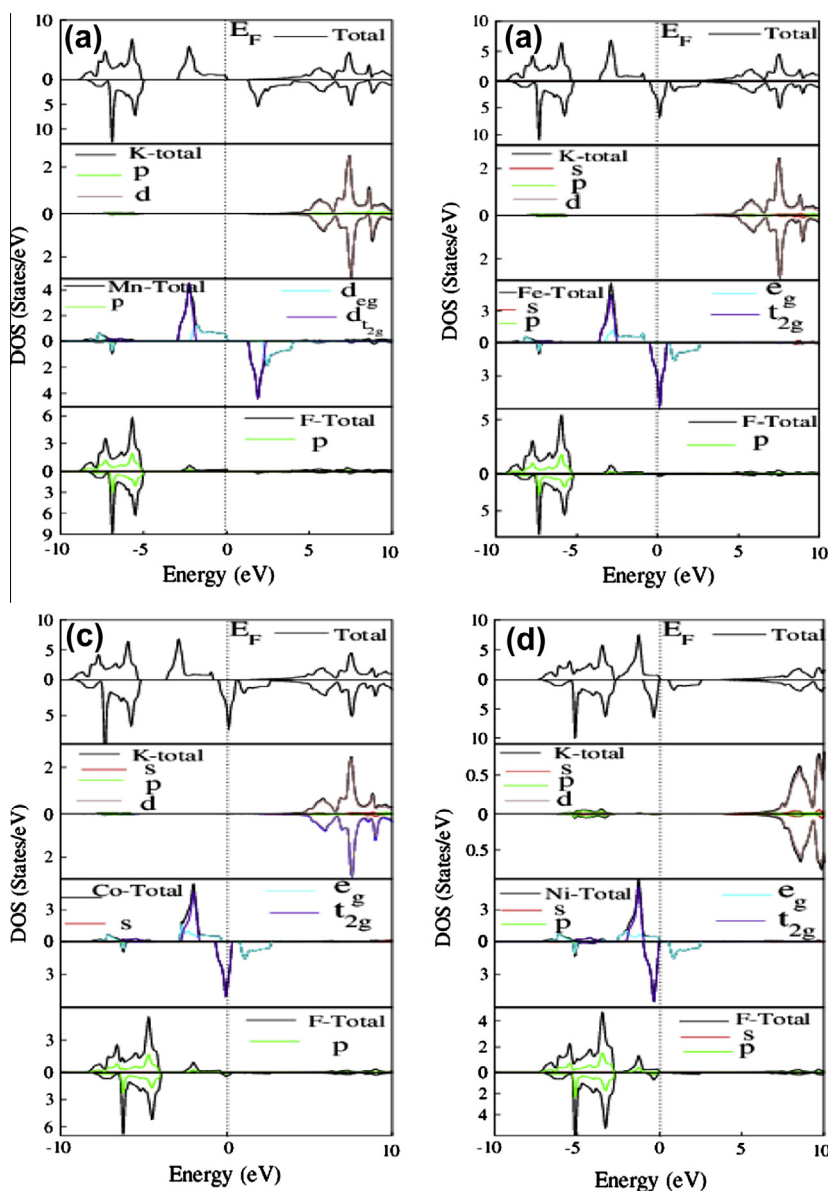


Fig. 2. Spin dependent total and partial density of states KMnF_3 (a), KFeF_3 (b), KCoF_3 (c) and KNiF_3 (d).

in Figs. 1 and 2, respectively. From Fig. 1, a semiconductor behavior can be seen in KMnF_3 and KNiF_3 with majority and minority spin channels while KFeF_3 and KCoF_3 are half metallic and being semiconductors with majority spin channel and metals with spin minority channel. This situation in KFeF_3 and KCoF_3 indicates typical half-metallic ferromagnetism with 100% spin polarization at Fermi level (E_F). Our results show that the band gap increases in going from Mn to Ni. The increase in the band gap from Mn to Ni is due to the decrease in the hybridization of 3d orbital of M ($M = \text{Mn, Fe, Co and Ni}$) and F-2p.

The densities of states (Fig. 2) of these compounds are plotted in the energy range from -20 eV to 20 eV. The main contributions in the total density of states are due to K: 3s,3p,3d, Mn: 3s,3p,3d, Fe: 3s,3p,3d, Co: 3s,3p,3d, Ni: 3s,3p,3d and F: 2s,2p states. Following Fig. 2, we should emphasize that there are four distinct bands in the density of electronic states separated by gaps. The lowest band from the left is composed by K-3p states. The bands below the Fermi level (E_F) are known as valence bands. The upper and lower valence bands are mainly composed of M-d states. The main spin polarization of the upper valence band takes place across the Fermi level. The conduction band, which is above the Fermi level, is mainly composed of K-3d, M-d and F-2p states.

In the cubic structure of KMnF_3 ($M = \text{Mn, Fe, Co and Ni}$), M atom is situated at the center of the octahedron surrounded by six oxygen ions, forming MF_6 octahedral. In the octahedron, the positively charged M atom attracts the negatively charged fluorine atoms. The electrons are arranged in the octahedron in such a fashion that F-2p states are completely filled and the M-3d states are partially filled. The densities of states for M- e_g and M- t_{2g} states in KMnF_3 ($M = \text{Mn, Fe, Co and Ni}$) are shown in Fig. 2. It is clear from Fig. 2 that t_{2g} states are lower in energy than e_g states and hence the overlapping of e_g with F-2p is stronger. Crystal fields are generated in these compounds because of the Coulombic repulsion between the electrons of M-3d states and F-2p states [44]. In cubic symmetry this repulsion causes splitting by degenerating M-3d states into two non-degenerate t_{2g} and e_g states.

Charge density of KMnF_3 ($M = \text{Mn, Fe, Co and Ni}$) for (1 1 0) planes is displayed in Fig. 3. Our predictions show that the Mn, Fe, Co and Ni charge density is spherical for spin up states, which illustrates that the M-3d levels are partially filled (shown in Fig. 2(a–d)). In the case of spin down states, the shape of M shifts from approximately spherical to dumbbly, which indicates ionic interactions with F. Electron density distribution indicates overlapping of states in Mn, Fe, Co and fluorine and explains the covalent nature of bond, while the nature of bond between Mn–F, Fe–F, Co–F, Ni–K is ionic. Fig. 2 shows that the e_g and t_{2g} states of M ($M = \text{Mn, Fe, Co and Ni}$) hybridizes strongly with the 2p state of F.

3.4. Magnetic properties

To study the magnetic properties of KMnF_3 ($M = \text{Mn, Fe, Co and Ni}$) compounds, their ferromagnetic and anti-ferromagnetic structures are optimized by minimizing the total energy of the unit cell with respect to the variation in the unit cell volume. We have found that the ferromagnetic state is energetically lower than the anti-ferromagnetic state. Furthermore, the magnetic properties of cobalt based perovskites depends on the spin state of Co^{2+} , Co^{3+} , Co^{4+} (HS, IS or LS) and the existence of indirect exchange interaction [45,46].

The calculated total, local and interstitial magnetic moments for KMnF_3 ($M = \text{Mn, Fe, Co and Ni}$) are given in Table 3. Our calculations show that the magnetic moments of Mn, Fe, Co and Ni are $4.41 \mu\text{B}$, $3.56 \mu\text{B}$, $2.65 \mu\text{B}$, $1.73 \mu\text{B}$ for KMnF_3 , KFeF_3 , KCoF_3 and KNiF_3 , respectively. The difference in the magnetic moments is due to the transfer of electrons from M to F atoms. One can also note that the magnetic moments decrease in going from Mn to Ni. Hence, the magnetic behavior becomes stronger in going from Ni to Mn. The magnetic moments of potassium for KMnF_3 ($M = \text{Mn, Fe, Co and Ni}$) are $0.0007 \mu\text{B}$, $-0.0016 \mu\text{B}$, $-0.0012 \mu\text{B}$ and $-0.0009 \mu\text{B}$, respectively. The negative signs of the magnetic moments of the K atom in KFeF_3 , KCoF_3 and KNiF_3 demonstrate that they are anti-parallel to Fe, Co and Ni and consequently reduce the net magnetic moments of the compounds. The positive values of the magnetic moments of the interstitial sites and F atoms confirm that they are parallel to the magnetic moments of transition metal elements M. The interstitial magnetic moments increase the overall magnetic nature of the compounds. The decrease in the magnetization from KMnF_3 to KNiF_3 is due to the hybridization of M-3d and F-2p states. The integer magnetic moment is also an important characteristic for half-metallic ferromagnets (HMFs). According to Slater–Pauling rule [47], the saturation magnetic moment of the HMFs is an integer and scales with the number of valence electrons. The calculated values of magnetic moment for KMnF_3 , KFeF_3 ,

Table 3

Calculated total (M^T), local and interstitial (m^{inst}) magnetic moments in the units of (μB) for KMnF_3 ($M = \text{Mn, Fe, Co and Ni}$).

Site	KMnF_3	KFeF_3	KCoF_3	KNiF_3
m^{inst}	0.3327	0.1523	0.0566	0.0176
m^K	0.0006	-0.0016	-0.0012	-0.0009
m^{M}	4.4336	3.5605	2.6561	1.7308
m^{F}	0.0779	0.0964	0.0963	0.0841
M^T	5.0006	4.0004	3.0004	1.9999

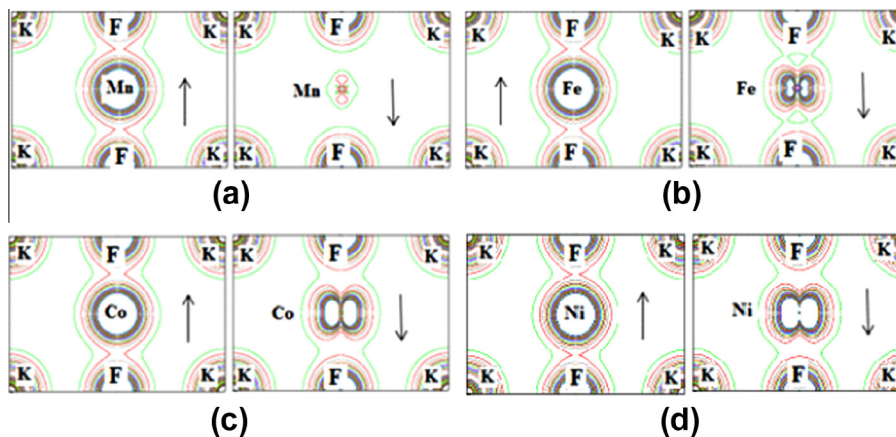


Fig. 3. Charge density for the spin-up and spin-down states of (1 1 0) plane of KMnF_3 (a), KFeF_3 (b), KCoF_3 (c) and KNiF_3 (d) perovskites.

KCoF₃ and KNiF₃ are 5.00 μB, 4.00 μB, 3.00 μB and 1.99 μB, respectively, which clearly indicates the ferromagnetic behavior of the herein studied compounds.

4. Conclusion

Structural, elastic, chemical bonding, electronic and magnetic properties of the KMnF₃, KFeF₃, KCoF₃ and KNiF₃ compounds are predicted by using the full-potential linearized augmented plane wave (FP-LAPW) method within the density functional theory (DFT). Calculated structural parameters through DFT and analytical method are in excellent agreement to the experimental measurements. Compounds are elastically stable, while KMnF₃ is ductile and the remaining compounds are found to be brittle. KMnF₃ and KNiF₃ are indirect band gap semiconductors in both spin channels while KFeF₃ and KCoF₃ are half metallic and being semiconductors with majority spin channel and metals with spin minority channel. The band gap increases from Mn to Ni in KMF₃. Compounds show mixed ionic and covalent bonding. All the compounds show ferromagnetic behavior. Due to half metallicity and ferromagnetic behavior these compounds can be used for spintronic applications.

Acknowledgements

Authors (Khenata, Bin Omran and Alahmed) acknowledge the financial support by the Deanship of Scientific Research at King Saud University for funding the work through the Research Group Project NO RPG-VPP-088. For A.H.Reshak the result was developed within the CENTEM project, reg. no. CZ.1.05/2.1.00/03.0088, cofunded by the ERDF as part of the Ministry of Education, Youth and Sports OP RDI programme.

References

- [1] H. Ohno, A. Sher, F. Matsuka, A. Oiwa, A. Eudo, *Appl. Phys. Lett.* 69 (1996) 363.
- [2] K.M. Wong, *Jpn. J. Appl. Phys.* 48 (2009) 085002.
- [3] C.N.R. Rao, B. Raveau (Eds.), *Transition Metal Oxides*, VCH Publishers, New York, 1995.
- [4] M.G. Brik, G.A. Kumar, D.K. Sardar, *Mater. Chem. Phys.* 136 (2012) 90.
- [5] M. Eibschutz, H.J. Guggenheim, S.H. Wemple, I. Camlibel, M. Didomenico, *Phys. Lett. A* 29 (1969) 409.
- [6] A.H. Cooke, D.A. Jones, J.F.A. Silva, M.R. Weils, *J. Phys. C: Solid State Phys.* 8 (1975) 4083.
- [7] R.A. Heaton, C.C. Lin, *Phys. Rev. B* 25 (1982) 3538.
- [8] G.G. Yakobson, N.E. Akhmetova, *Synthesis* 1983 (1983) 169.
- [9] M. Sahnoun, M. Zbiri, C. Daul, R. Khenata, H. Baltache, M. Driz, *Mater. Chem. Phys.* 91 (2005) 185.
- [10] E.N. Maslen, N. Spaldaccini, T. Ito, F. Marumo, K. Tanaka, Y. Satow, *Acta Crystall. B* 49 (1993) 632.
- [11] A. Okazaki, Y. Suemune, *J. Phys. Soc. Jpn.* 16 (1961) 671.
- [12] M. Abdul, S.L. Yeon, *Adv. Inf. Sci. Serv. Sci.* 2 (2010) 3.
- [13] W. Kohn, L.S. Sham, *Phys. Rev. A* 140 (1965) 1133.
- [14] C.A. Ullrich, *Phys. Rev. Lett.* 87 (2001) 093001.
- [15] O.K. Andersen, *Phys. Rev. B* 12 (1975) 3060.
- [16] K.M. Wong, S.M. Alay-e-Abbas, A. Shaikat, Y. Fang, Y. Lei, *J. Appl. Phys.* 113 (2013) 014304.
- [17] Z. Wu, R.E. Cohen, *Phys. Rev. B* 73 (2006) 235116.
- [18] K.M. Wong, S.M. Alay-e-Abbas, Y. Fang, A. Shaikat, Y. Lei, *J. Appl. Phys.* 114 (2013) 034901.
- [19] P. Blaha, K. Schwarz, G.K.H. Madsen, D. Kvasnicka, J. Luitz, *WIEN2K: An Augmented Plane Wave Local Orbital Program for Calculating Crystal Properties*, Technische Universität, Wien, Austria, 2001.
- [20] J.L. Erskine, E.A. Stern, *Phys. Rev. Lett.* 30 (1973) 1329.
- [21] F. Birch, *Phys. Rev.* 7 (1947) 809.
- [22] R. Ubig, *J. Am. Ceram. Soc.* 90 (2007) 3326.
- [23] J. Lee, H. Shin, H. Chung, Q. Zhang, F. Saito, *Mater. Trans.* 44 (2003) 1457.
- [24] J.B. Goodenough, *Rep. Prog. Phys.* 67 (2004) 1915.
- [25] Roberto L. Moreira, D. Anderson, *J. Phys. Chem. Solids* 68 (2007) 1617.
- [26] N. Xu, H. Zhao, X. Zhou, W. Wei, X. Lu, W. Ding, F. Li, *Int. J. Hydrogen Energy* 35 (2010) 7295.
- [27] E. Schreiber, O.L. Anderson, N. Soga, *Elastic Constants and their Measurement*, McGraw-Hill, New York, 1973.
- [28] K.D. Reddy, P. Kistaiah, L. Iyengar, *J. Less Common Met.* 92 (1983) 81.
- [29] G. Vaitheeswaran, V. Kanchana, R.S. Kumar, A.L. Cornelius, M.F. Nicol, A. Svane, A. Delin, B. Johansson, *Phys. Rev. B* 76 (2007) 014107.
- [30] T. Seddik, R. Khenata, O. Merabiha, A. Bouhemadou, S. Bin-Omran, D. Rached, *Appl. Phys. A* 106 (2012) 645.
- [31] J. Wang, S. Yip, *Phys. Rev. Lett.* 71 (1993) 4182.
- [32] V. Tvergaard, J.W. Hutshinson, *J. Am. Ceram. Soc.* 71 (1988) 157.
- [33] W. Voigt, *Lehrbush der Kristallphysik*, Taubner, Leipzig, 1928.
- [34] A. Russ, *Angew. Mat. Phys.* 9 (1929) 49.
- [35] Z.J. Wu, E.J. Zhao, H.P. Xiang, X.F. Hao, X.J. Liu, J. Meng, *Phys. Rev. B* 76 (2007) 054115.
- [36] F. Peng, D. Chen, H. Fu, X. Cheng, *Phys. Stat. Sol. B* 71 (2009) 246.
- [37] B. Ghebouli, M.A. Ghebouli, M. Fatmi, A. Bouhemadou, *Solid State Commun.* 150 (2010) 1896.
- [38] H. Fu, D. Li, F. Peng, T. Gao, X. Cheng, *Comput. Mater. Sci.* 44 (2008) 774.
- [39] K. Kim, W.R.L. Lambrecht, B. Segal, *Phys. Rev. B* 50 (1994) 1502.
- [40] L. Kleinman, *Phys. Rev. B* 12 (1962) 2614.
- [41] D.G. Pettifor, *Mater. Sci. Technol.* 8 (1992) 345.
- [42] S.F. Pugh, *Philos. Mag.* 45 (1954) 823.
- [43] I.N. Frantsevich, F.F. Voronov, S.A. Bokuta, *Elastic Constants and Elastic Moduli of Metals and Insulators Handbook*, in: I.N. Frantsevich (Ed.), *Naukova Dumka, Kiev*, 1983, pp. 60–180.
- [44] S. Sugano, Y. Tanabe, H. Kamimura, *Multiplets of Transition-Metal Ions in Crystals*, vol. 70, first ed., Academic Press, New York, London, 1970.
- [45] C. Zener, *Phys. Rev.* 82 (1951) 403.
- [46] P.W. Anderson, H. Hasegaw, *Phys. Rev.* 100 (1955) 675.
- [47] J.C. Slater, *Phys. Rev.* 49 (1936) 537.